

Enhancing next token prediction based pre-training for jet foundation models

Joschka Birk,^{1,*} Anna Hallin,^{1,†} Gregor Kasieczka,^{1,‡} Nikol Madzharova,^{1,§} Ian Pang,^{2,¶} and David Shih^{2,**}

¹*Institut für Experimentalphysik, Universität Hamburg, 22761 Hamburg, Germany*

²*NHETC, Dept. of Physics and Astronomy, Rutgers University, Piscataway, NJ 08854, USA*

Next token prediction is an attractive pre-training task for jet foundation models, in that it is simulation free and enables excellent generative capabilities that can transfer across datasets. Here we study multiple improvements to next token prediction, building on the initial work of OmniJet- α . Instead of tokenizing particles and subsequently only using the token-ID as the model input for both the generative and the classification task, we adopt a hybrid setup, which allows us to use continuous feature vectors as model input while only using token-IDs in the next token prediction target. Secondly, we explore a combined pre-training strategy that combines masked particle modeling and generative learning objectives. Taken together, these changes greatly improve the performance in downstream classification tasks without any loss in generative performance.

I. INTRODUCTION

Foundation models [1] applied to high energy physics (HEP) data have recently received substantial interest, motivated by their ability to generalize to previously unseen datasets and tasks. Jet physics in particular has been a key target for the development of HEP foundation models (see [2] for a recent review), due to its wide practical relevance across LHC and future collider experiments, and its well-established role as benchmark for machine learning (ML) algorithms [3].

Much of the activity so far in the development of foundation models for jets has centered around exploring different approaches to pre-training and fine-tuning in order to optimize the expressivity of the learned representations and the performance on downstream tasks. For example, there have been many different proposals for the pre-training objective. These range from predicting a missing entry, based either on masking [4–8] or next token prediction [9], to classification [10–14], data augmentation and contrastive learning [15, 16] or a combination of tasks [11–13]. Despite all these efforts, it remains unclear to what extent different pre-training methods produce representations that align well with the demands of downstream tasks. Different pre-training objectives correlate strongly with performance on downstream tasks: for instance some approaches enable classification but not generation or vice versa. This is clearly an unsatisfactory situation for the HEP foundation model paradigm.

Another dividing line is the reliance on ground-truth information in the training phase, which determines whether they can in-principle be trained using data or whether simulation is required. While simulation-based approaches [10–15] can leverage supervised training on high-fidelity simulations, simulation-free approaches [4–9, 16, 17] have the potential to be trained directly on the copious amounts of real LHC data (which far outnumbers simulated data).

This work focuses on OmniJet- α [9] as the only model with demonstrated generative capabilities and transfer learning between tasks that can be fully trained on data. However, these advantages so far came at a price, namely a sub-optimal performance when considering downstream classification tasks. Here, we identify and improve upon two limitations of the original OmniJet- α approach, stemming from it being an autoregressive GPT-like model. In both cases, we modify the architecture to align more closely with the nature of our physics data, while maintaining the attractive simulation-free and generation-capable properties.

First, we show that using tokenized input during the classifier training harms classification ability. The main reason for tokenization is that it improves generative pre-training and generative downstream performance. However, due to information loss and possible artifacts [18], tokenization might not be the most optimal choice. To circumvent these issues, we present an improved hybrid setup for next token prediction based pre-training, where the input feature vectors are continuous while the pre-training targets remain token-IDs. Allowing for continuous input significantly increases the classification capabilities of our model, while keeping the token-IDs as targets for the pre-training preserves the generative performance.

Second, we revisit the pre-training task. It is known from natural language processing (NLP) that models based on causal attention and next token prediction excel at generation, whereas bi-directional approaches using masking produce rich contextual embeddings. Recent works that have focused on combining the two training objectives include [19–24]. While OmniJet- α has strong generative capabilities due to its next token prediction (NTP) pre-training, we hypothesize that tasks such as jet classification require a contextual understanding of the jet constituents which may be better served by bi-directional pre-training like masked particle modeling (MPM) [4, 5] and other methods based on masked prediction [6–8]. Inspired by the results from the NLP literature, we investigate the performance of both NTP and MPM during pre-training and subsequent fine-tuning to classification, including a setup that combines both training objectives. We show how pre-training on both next and masked token prediction simultaneously leads to a drastic improvement of downstream classification performance, while maintaining the

* joschka.birk@uni-hamburg.de

† anna.hallin@uni-hamburg.de

‡ gregor.kasieczka@uni-hamburg.de

§ nikol.madzharova@studium.uni-hamburg.de

¶ ian.pang@physics.rutgers.edu

** shih@physics.rutgers.edu

generative capabilities.

The rest of this paper adheres to the following structure: [Section II](#) describes the used datasets, reviews the original OmniJet- α method and its limitations, and details the modifications we introduce to address them. [Section III](#) reports the performance gains from (i) adapting to a continuous model input and (ii) updating the pre-training objective to combine next token and masked token prediction. Our conclusions are presented in [Section IV](#). Additional details, analyses and ablation studies are provided in [Sections A](#) to [D](#).

II. SETUP

The model is implemented in PYTORCH [25] and LIGHTNING [26]. Furthermore, we use the open source software libraries in Refs. [27–38]. The overall architecture of the model is similar to the one used in OmniJet- α , with a few minor updates outlined in [Section A](#).

A. Datasets

Two datasets are used in our studies: the JetClass [10, 39] dataset and the top tagging dataset [3, 40].

The JetClass dataset contains 100 M training jets from simulated proton-proton collisions at the LHC. It contains ten different jet types, with the individual jet types corresponding to one background jet type (quark- or gluon-initiated jets) and nine signal jet types where the jet originates from the decay of a top quark, a W , Z or Higgs boson. The individual jet types are: q/g , $t \rightarrow bq\bar{q}'$, $t \rightarrow b\ell\nu$, $W \rightarrow qq'$, $Z \rightarrow q\bar{q}$, $H \rightarrow b\bar{b}$, $H \rightarrow c\bar{c}$, $H \rightarrow gg$, $H \rightarrow 4q$, $H \rightarrow \ell\nu qq'$. The events are simulated with MadGraph5_aMC@NLO [41]. Pythia8 [42, 43] is used for parton showering and hadronization, and a simplified detector simulation is performed with Delphes [44] using the CMS [45] detector card. The particles are clustered with the anti- k_T [46] algorithm with a distance parameter of $R = 0.8$, and only jets with a transverse momentum in the range of $500 \text{ GeV} < p_T < 1000 \text{ GeV}$ and a pseudorapidity of $|\eta| < 2.0$ are included in the dataset. Further details on the JetClass dataset can be found in [10].

The top tagging dataset contains q/g jets as well as $t \rightarrow bq\bar{q}'$ jets. This dataset is significantly smaller than the JetClass dataset, with 1.2 M training jets. It contains jets extracted from LHC events that were simulated with Pythia8 [42, 43] and Delphes [44] using the ATLAS [47] detector card. The jets are clustered with the anti- k_T [46] algorithm with a distance parameter of $R = 0.8$, and are required to have $|\eta| < 2.0$ and a transverse momentum in the range of $550 \text{ GeV} < p_T < 650 \text{ GeV}$.

B. Original OmniJet- α method

An overview of the method of the original work is shown in [Figure 1](#) (upper row). In the original OmniJet- α work jet

constituents are first tokenized with a vector quantized autoencoder (VQ-VAE) [4, 48, 49] to obtain a discrete representation of the continuous input features, in the following referred to as *token-IDs*, denoted as t_i . The pre-training is performed on the generative task, which is trained with NTP. Afterwards, the integer number token-IDs are used as input for both the generative and classification tasks.

A key advantage of the original OmniJet- α setup is that generative pre-training produces good generative models that can be transferred to different datasets with minimal fine-tuning [17], and earlier studies have shown that such models are directly useful for anomaly detection [11, 12, 50]. Beyond this immediate utility, the same pre-training was shown to significantly improve classification performance relative to training from scratch. However, the absolute classification performance obtained in this way still falls short of the current state-of-the-art. As we will show with the modifications to OmniJet- α detailed in the next subsection, this performance gap arises from the original design choice to use the discrete token-IDs as model input, as well as from the limited contextual representation learned under a NTP objective.

C. Modifications

1. Continuous-input next-token prediction

The main advantage of using continuous input vectors is that the downstream classification task can operate directly on the full resolution feature vectors \vec{c}_i , ensuring that the model does not suffer from tokenization-induced loss of information in this task. With this goal of improving downstream classification performance, we use continuous feature vectors as model inputs while token-IDs serve only as next token prediction targets, following the hybrid setup employed in prior works. The general framework is shown in [Figure 1](#) (bottom row): during pre-training, the model acts on pseudo-continuous feature vectors, denoted in [Figure 1](#) as \vec{d}_i , which refers to the continuous representations of the tokenized inputs (i.e. the decoded token-IDs). During autoregressive jet generation, the decoding of token-IDs is integrated into the autoregressive generation loop. Note that this additional decoding step is not needed during training, as the whole sequence of particle tokens is fed to the model at once.

2. Masked token prediction

Following masked modeling approaches in natural language processing and computer vision [51–56], masked modeling was introduced for jet physics in the form of Masked Particle Modeling (MPM) [4, 5]. Although MPM does not produce a generative model out of the box, it has demonstrated competitive classification performance. Since the pre-training strategies of MPM and our method differ mainly in whether the model predicts masked particles or the next particle, it is a close relative to our method and we include it in our setup in

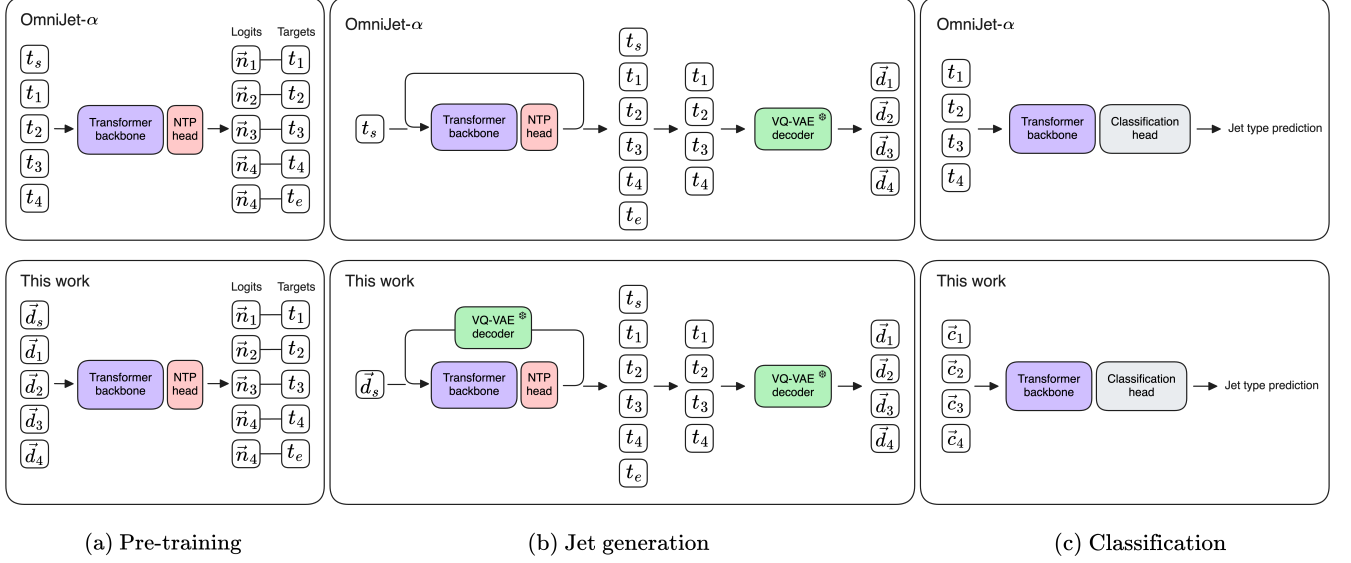


FIG. 1. The high-level architecture of the OmniJet workflow: (a) the pre-training based on next token prediction, (b) the generative model obtained from unsupervised pre-training and (c) the classification model obtained from supervised fine-tuning. Our new approach uses continuous feature vectors as input, both for the generative and classification tasks. Token-IDs are shown as t_i , with t_s corresponding to a start token and t_e corresponding to an end token. The continuous feature vectors are shown as \vec{c}_i , and the pseudo-continuous feature vectors (i.e. the decoded token-IDs) are shown as \vec{d}_i . In the continuous input case, the start token is a trainable embedding \vec{d}_s .

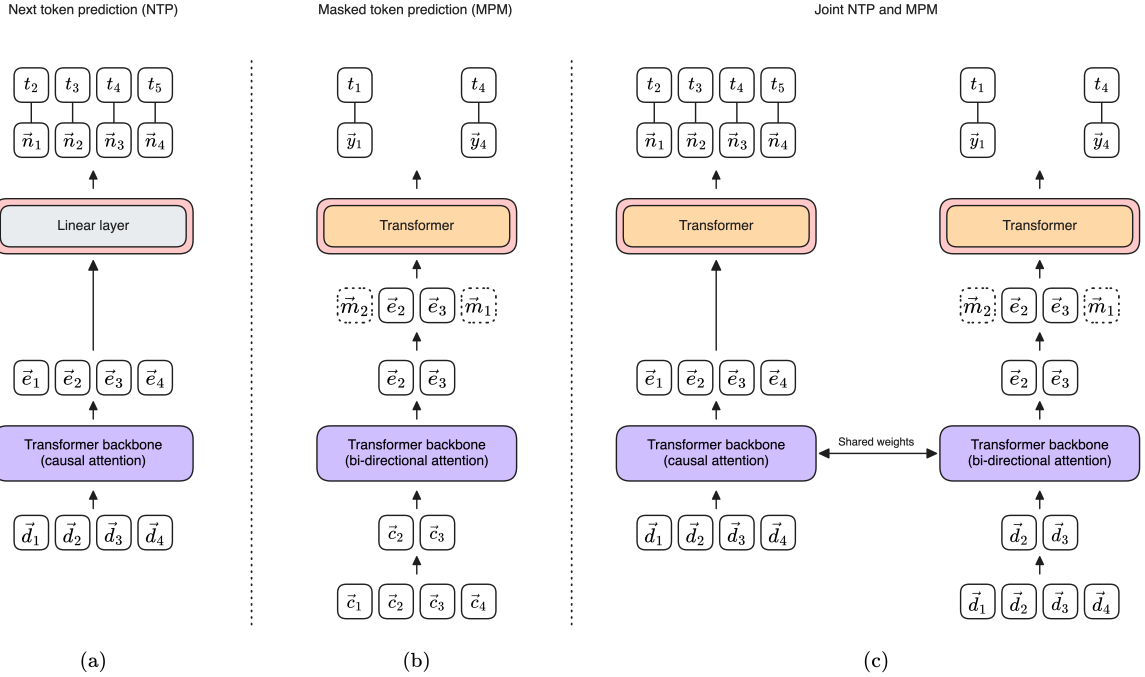


FIG. 2. Schematic overview of the different pre-training strategies: (a) next token prediction (NTP), (b) masked token prediction (MPM) [4, 5], and (c) joint NTP and MPM. Token-IDs are shown as t_i , continuous feature vectors as \vec{c}_i , pseudo-continuous feature vectors as \vec{d}_i , the mask embeddings as \vec{m}_i . The vectors \vec{e}_i represent the backbone output and \vec{n}_i and \vec{y}_i represent the next and masked token predictions, respectively. The particles are not p_T -sorted, but with positional encoding the information of the p_T -order within the masked subset is recovered: in this example, the first masked particle (position 1) is assumed to have smaller p_T than the second masked particle (position 4), which is why they are re-introduced as \vec{m}_2 and \vec{m}_1 respectively when using positional encoding.

order to study the effects of masked token versus next token prediction on the classification task performance.

In the MPM setup, shown in Figure 2b, a fraction of the input particles is removed from the input sequence before being passed to the transformer backbone. After the backbone, the masked particles are reinserted into the sequence in the form of mask embeddings \vec{m}_i , which are trainable embeddings that are initialized with Gaussian noise and are learned during training. Positional encoding is applied to these reinserted mask embeddings. Here, the index i refers to the position of a masked particle in the p_T -sorted subset of masked particles. That is, the i^{th} highest p_T masked particle is reintroduced to the jet (after the backbone) as \vec{m}_i . The model head is then tasked to predict the token-ID of the masked positions. The main difference in our implementation compared to the original MPM works is that we use a significantly smaller backbone model, which is described in more detail in Section A.

A natural question is whether the benefits of MPM stem from its objective (predicting masked tokens) or some difference in the neural network architecture. The main difference is the use of bi-directional attention in MPM (required by the permutation symmetry that comes with treating the jets as point clouds), compared with the causal attention used in NTP (required by treating the jets as sequences). To address this, we implement a version of MPM that uses a causal attention mask in the backbone transformer as well as in the model head, in the following referred to as *MPM-Causal*. This setup preserves the causal attention structure of NTP while changing only the prediction objective, allowing for a controlled comparison between the two factors. A masking rate of 40% is used in all MPM(-Causal) trainings as this was found to be the optimal masking rate in [5].

3. Joint next and masked token prediction

To investigate if the advantages of both next and masked token prediction can be combined, we implement a joint pre-training. An illustration of the joint setup is shown in Figure 2c. This joint pre-training is realized by having two model heads, predicting the next token logits and the masked token logits, respectively. The two individual loss terms are simply added without any further modification. Two backbone forward passes are performed during pre-training. The forward pass for the masked token prediction is performed the same way as for pure MPM, i.e. with bi-directional attention and with positional encoding. For the next token prediction all jet constituents are used as input and the causal mask is applied. Furthermore, so as to not force the NTP backbone to align its output too strongly with the generative task, we use a transformer in the NTP head in addition to the simple unembedding layer that the original OmniJet- α was trained with. This allows the model to further modify the backbone representation with causal attention before projecting the representation to next token logits.

III. RESULTS

We pre-train the backbone on the whole 100 M-jet training set of the JetClass dataset for each pre-training strategy. Afterwards, we evaluate the quality of the generative model (in cases where the pre-training involves NTP) and quantify the effectiveness of the different pre-training strategies by fine-tuning the pre-trained models on jet classification. Unless otherwise specified we restrict the set of input features to the kinematic features (particle p_T , $\Delta\phi$ and $\Delta\eta$), as the other features included in the JetClass dataset are not available in the top tagging dataset¹.

A. Token-ID input vs. continuous input

We first verify that the change of input structure from token-IDs to continuous feature vectors can be accomplished without sacrificing the performance of the corresponding generative model. The jet and particle-level distributions obtained from generated jets of the two different input types is compared to their target distributions in Figure 3. For both models the particle-level distributions of the generated jets show very good agreement with the jets from the JetClass dataset and small deviations from the target distribution. The change in input structure (continuous feature vectors instead of token-IDs) thus doesn't harm the performance of the generative model.

The positive effect of the continuous input on the classification performance is shown in Figure 4a for in-distribution and in Figure 4b for out-of-distribution transfer learning. For in-distribution transfer learning, we fine-tune the model on multi-class classification (10 classes) on the JetClass dataset with training dataset sizes between 1 k and 100 M jets. As expected, the *from scratch* model, i.e. the baseline model without any pre-training, performs significantly better with continuous input features than with token-ID inputs for all dataset sizes. This demonstrates that the tokenization alone significantly harms the classification performance.

The pre-trained models improve the performance compared to their respective from-scratch models in both the token-ID and the continuous case. In the token-ID input case, the pre-trained model outperforms the from-scratch model for all dataset sizes except for the largest dataset size. In the largest dataset size regime, at 100 M jets, the from-scratch model catches up with the fine-tuned model, which indicates that the model has seen enough training data to learn the relevant features from scratch and using the pre-trained weights as initialization does not provide a benefit anymore. Meanwhile, in the continuous input case, we still observe a performance gain from generative pre-training for small dataset sizes, while the

¹ We investigate the effect of extending the feature set to include the particle-ID and trajectory displacement information of the jet constituents for a model pre-trained with NTP using continuous inputs, and observe, as expected, a significant improvement in the classification capabilities. This study is shown in Section C.

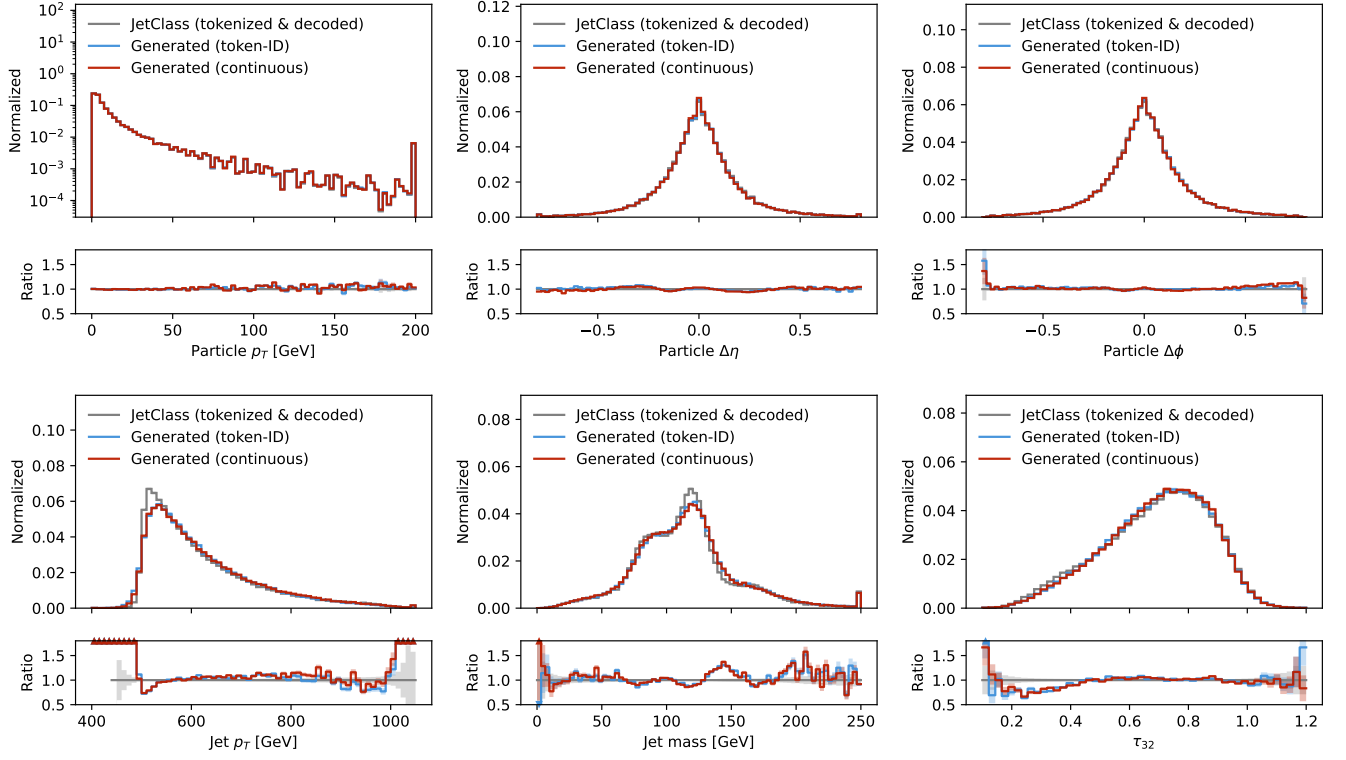


FIG. 3. Comparison of the jets that are generated by the token-ID-input and the continuous-input model, as well as the jets from the JetClass dataset on particle-level (top row) and jet-level (bottom row). The first and last bins show the under- and overflow bins, respectively. The jets shown for the JetClass dataset are tokenized and subsequently decoded, representing the target of the generative model.

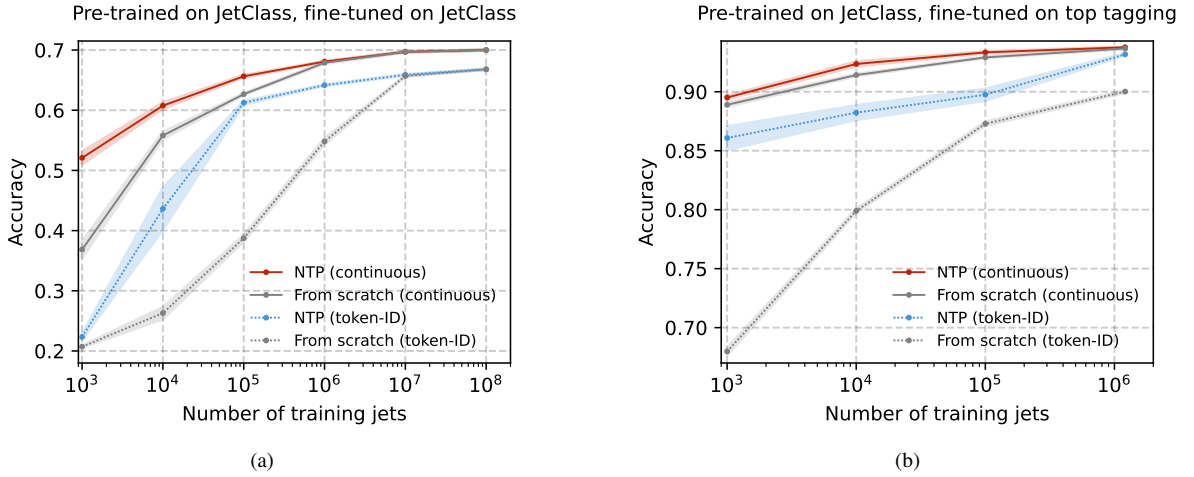


FIG. 4. Comparison of token-ID input vs. continuous input classification performance: (a) for multi-class classification performance on the JetClass dataset (all 10 jet types, in-distribution transfer learning) and (b) for binary classification performance on the top tagging (out-of-distribution transfer learning) as a function of the number of training jets.

from-scratch and fine-tuned model converge to a similar performance for training dataset sizes of 1 M jets or more.

For the out-of-distribution transfer learning we fine-tune the model on the binary classification task on the top tagging dataset. The dataset range for this study is between 1k

and 1.2 M jets, with the latter being the full training dataset size of this dataset. We see very similar trends as for in-distribution transfer learning, with a clear performance gain when using continuous input features instead of token-ID input features. In this case, generative pre-training offers an

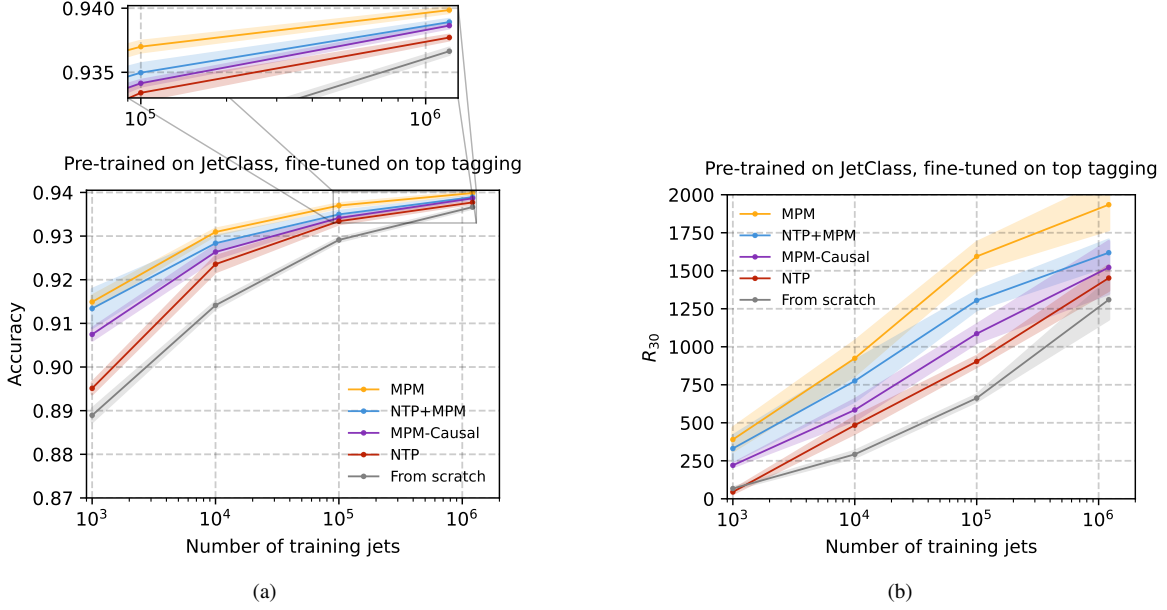


FIG. 5. Classification performance on the top tagging dataset with different pre-training strategies: (a) the classifier accuracy and (b) the background (q/g -jet) rejection at 30 % signal (top-jet) efficiency. All models use continuous feature vectors as input.

improvement over the from-scratch baseline for the whole dataset range, both for the token-ID input and the continuous input case. While the continuous input classifier presented here is still outperformed by jet taggers that pre-train in a supervised manner directly on a classification task, like ParT [10], L-GATr [57, 58] or OmniLearned [13], this is expected as the studies presented here use a plain transformer architecture without physics-inspired interaction features or more involved, Lorentz-equivariant model architectures, and is also pre-training completely without labels.

B. Comparison of different pre-training objectives

For the comparison of different pre-training strategies (NTP, MPM and joint), we pre-train with continuous inputs on the JetClass dataset with the kinematic-only feature set and fine-tune on the top tagging dataset. The results of this comparison are shown in Figure 5. All investigated pre-training strategies lead to an improvement over the baseline for the whole range of training dataset sizes, except for the R_{30} metric² at a training dataset size of 1000 jets where the fine-tuned NTP model performs slightly worse than the from-scratch baseline. This could be due to the fact that the difference between the pre-training task (next token prediction) and the target task (classification) is too large, with the model not being able to adjust to the target task with only 1000 training jets during fine-tuning. Additional evidence for this interpretation is provided in Appendix D, where fine-tuning with a fixed

backbone shows that NTP-pretrained representations are substantially less aligned with classification than those obtained from MPM or joint pre-training.

While pre-training with NTP leads to a significant improvement over the from-scratch baseline, it is outperformed by the other pre-training strategies with the best performance being achieved by MPM. The MPM-Causal setup (i.e. predicting masked tokens with causal attention) performs similarly to the next token prediction setup. This indicates that the classification performance gains seen in MPM are not solely due to the masked prediction objective itself. The different attention mechanisms (bidirectional vs. causal) also plays an important role. Apparently, bi-directional attention allows the model to develop a contextual understanding in a better way than causal attention does.

The joint pre-training clearly outperforms the standard NTP pre-training and results in a classification performance close to that of pure MPM. At the same time, as shown in Figure 6, we observe that the generative capabilities of our model are not reduced by the joint training on NTP and MPM, with both models showing very similar agreement with the target distribution, both on particle level and on jet level.

IV. CONCLUSION

When transplanting the methods of transformer-based foundation models from their origins in the modeling of language to their new home in solving problems in jet physics, their assumptions need to be revisited. For example, while the concept of tokens naturally fits data that can be seen as composed from discrete elements — such as words or word fragments — another representation might suit the typically

² The R_{30} metric is the background rejection at 30 % signal efficiency.

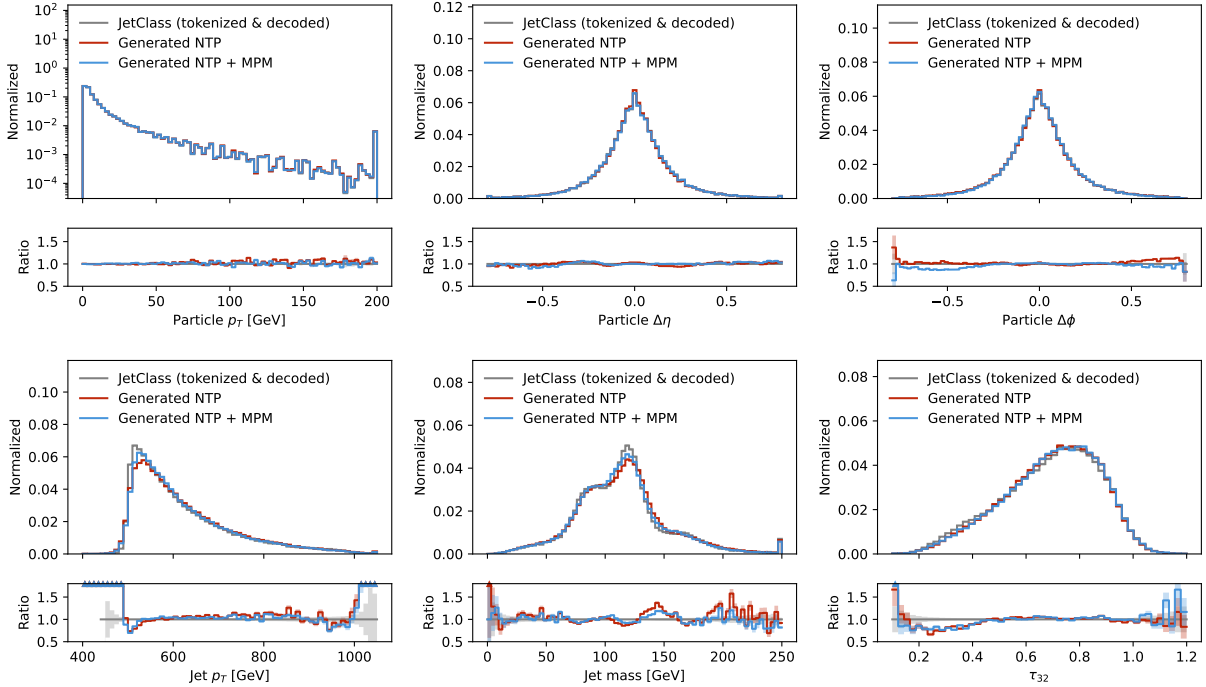


FIG. 6. Comparison of the generative models trained with NTP only vs. joint NTP and MPM. The jets shown for the JetClass dataset are tokenized and subsequently decoded, representing the target of the generative model.

continuous, high resolution read-outs of modern particle detectors better. Moreover, it is not yet clear which pre-training strategy or strategies best fit the specific downstream tasks that are of interest to particle physicists.

In this work, we have investigated these two questions: the effect of tokenizing inputs, and of setting useful pre-training tasks. We first found that a hybrid approach with respect to tokenization can combine the best of both worlds. While the learning target for the generative pre-training step remains tokenized, it uses continuous feature vectors with limited resolution (obtained by the decoder of the VQ-VAE that created the tokens in the first place) as input. This allows the model to keep its strong generative performance, while not restricting the input format to be tokenized. The model can then be fine-tuned directly to classify using full-resolution continuous inputs, leading to drastic improvement of classification performance as it is no longer limited to using token-IDs as input.

Next, we turned to the fairly subtle difference between predicting subsequent tokens (next token prediction, NTP) and predicting randomly masked-out tokens (masked particle modeling, MPM). Naively, the difference seems marginal. However, empirically, a non-trivial difference in performance can be observed. To better understand this behavior, we introduced the causally-masked version of MPM, allowing particles to only attend to their predecessors and thereby blocking the bi-directional attention. As this causal MPM version performs almost on-par with the generative NTP approach, one can conclude that the bi-directional attention of MPM plays a major role in aligning the learned representation for the clas-

sification task.

Finally, we investigated a joint NTP/MPM pre-training scheme and showed that it is both possible and beneficial: combining both objectives improves on the downstream classification performance while maintaining the generative fidelity of pure NTP training. Evidently, enhancing the learned representation via some injection of MPM training does not adversely affect the generative power of NTP pretraining.

As both generative and predictive tasks are crucial applications of a successful foundation model of jet physics, the hybridization options developed in this work will aid the successful implementation of such a model. Beyond the ideas considered here, one might further investigate whether other tokenization schemes could yield performances surpassing the VQ-VAE — especially as the number of features is further increased. Alternatively, one could explore whether generation could even be achieved while fully avoiding discrete tokens [59]. Finally, these hybrid ideas could also point towards approaches that include physical priors more explicitly, while retaining the flexibility of foundation models.

ACKNOWLEDGEMENTS

The authors thank Oz Amram, Darius Faroughy, Michael Krämer, Alexander Mück, and Humberto Reyes-Gonzalez for stimulating exchanges regarding foundation models. We would also like to thank Thorsten Buss for valuable discussions throughout this project. JB, AH, GK, and NM are

supported by the DFG under the German Excellence Initiative – EXC 2121 Quantum Universe – 390833306, and by PUNCH4NFDI – project number 460248186. IP and DS are supported by DOE grant DOE-SC0010008. We also acknowledge support via the SciFM consortium (05D25GU4) funded by the German Federal Ministry of Research, Technology, and Space (BMFTR) in the ErUM-Data action plan as well as the Hamburg VISTA/VISOR — Virtual Initiative for Science & Technology in AI — network. This research was supported in part by grant NSF PHY-2309135 to the Kavli Institute for Theoretical Physics (KITP).

For this work the HPC-cluster Hummel-2 at University of

Hamburg was used. The cluster was funded by Deutsche Forschungsgemeinschaft (DFG, German Research Foundation) – 498394658. Additionally, we acknowledge support from the Maxwell computational resources at Deutsches Elektronen-Synchrotron DESY, Hamburg, Germany.

CODE

The code for this paper is available at github.com/uhh-pd-ml/enhancing-ntp4jets.

-
- [1] R. Bommasani *et al.*, On the opportunities and risks of foundation models, *arXiv* (2021), 2108.07258.
 - [2] A. Hallin, Foundation models for high-energy physics (2025) *arXiv:2509.21434 [hep-ph]*.
 - [3] A. Butter *et al.*, The Machine Learning landscape of top taggers, *SciPost Phys.* **7**, 014 (2019), *arXiv:1902.09914 [hep-ph]*.
 - [4] T. Golling, L. Heinrich, M. Kagan, S. Klein, M. Leigh, M. Osadchy, and J. A. Raine, Masked particle modeling on sets: towards self-supervised high energy physics foundation models, *Mach. Learn. Sci. Tech.* **5**, 035074 (2024), *arXiv:2401.13537 [hep-ph]*.
 - [5] M. Leigh, S. Klein, F. Charton, T. Golling, L. Heinrich, M. Kagan, I. Ochoa, and M. Osadchy, Is Tokenization Needed for Masked Particle Modelling?, *Machine Learning: Science and Technology* **6**, 025075 (2025), *arXiv:2409.12589 [hep-ph]*.
 - [6] S. Katel, H. Li, Z. Zhao, F. Mokhtar, J. Duarte, and R. Kansal, Learning Symmetry-Independent Jet Representations via Jet-Based Joint Embedding Predictive Architecture, in *Machine Learning and the Physical Sciences: Workshop at NeurIPS 2024* (2024) *arXiv:2412.05333 [hep-ph]*.
 - [7] A. J. Wildridge, J. P. Rodgers, E. M. Colbert, Y. yao, A. W. Jung, and M. Liu, Bumblebee: Foundation Model for Particle Physics Discovery, in *38th conference on Neural Information Processing Systems* (2024) *arXiv:2412.07867 [hep-ex]*.
 - [8] J. Bardhan, R. Agrawal, A. Tilak, C. Neeraj, and S. Mitra, HEP-JEPA: A foundation model for collider physics using joint embedding predictive architecture, (2025), *arXiv:2502.03933 [cs.LG]*.
 - [9] J. Birk, A. Hallin, and G. Kasieczka, OmniJet- α : the first cross-task foundation model for particle physics, *Mach. Learn. Sci. Tech.* **5**, 035031 (2024), *arXiv:2403.05618 [hep-ph]*.
 - [10] H. Qu, C. Li, and S. Qian, Particle transformer for jet tagging, in *Proceedings of the 39th International Conference on Machine Learning*, Proceedings of Machine Learning Research, Vol. 162, edited by K. Chaudhuri, S. Jegelka, L. Song, C. Szepesvari, G. Niu, and S. Sabato (PMLR, 2022) pp. 18281–18292.
 - [11] V. Mikuni and B. Nachman, Solving key challenges in collider physics with foundation models, *Phys. Rev. D* **111**, L051504 (2025), *arXiv:2404.16091 [hep-ph]*.
 - [12] V. Mikuni and B. Nachman, Method to simultaneously facilitate all jet physics tasks, *Phys. Rev. D* **111**, 054015 (2025), *arXiv:2502.14652 [hep-ph]*.
 - [13] W. Bhimji, C. Harris, V. Mikuni, and B. Nachman, OmniLearned: A Foundation Model Framework for All Tasks Involving Jet Physics, (2025), *arXiv:2510.24066 [hep-ph]*.
 - [14] J. Ho, B. R. Roberts, S. Han, and H. Wang, Pretrained Event Classification Model for High Energy Physics Analysis (2024), *arXiv:2412.10665 [hep-ph]*.
 - [15] P. Harris, J. Krupa, M. Kagan, B. Maier, and N. Woodward, Resimulation-based self-supervised learning for pretraining physics foundation models, *Phys. Rev. D* **111**, 032010 (2025), *arXiv:2403.07066 [hep-ph]*.
 - [16] Z. Hao, R. Kansal, A. Gandrakota, C. Sun, N. Jennifer, J. Duarte, and M. Spiropulu, Rino: Renormalization group invariance with no labels (2025), *arXiv:2509.07486 [hep-ex]*.
 - [17] O. Amram, L. Anzalone, J. Birk, D. A. Faroughy, A. Hallin, G. Kasieczka, M. Krämer, I. Pang, H. Reyes-Gonzalez, and D. Shih, Aspen Open Jets: unlocking LHC data for foundation models in particle physics, *Mach. Learn. Sci. Tech.* **6**, 030601 (2025), *arXiv:2412.10504 [hep-ph]*.
 - [18] I. Pang, D. A. Faroughy, D. Shih, R. Das, and G. Kasieczka, SURFing to the Fundamental Limit of Jet Tagging, (2025), *arXiv:2511.15779 [hep-ph]*.
 - [19] A. Lv, K. Zhang, S. Xie, Q. Tu, Y. Chen, J.-R. Wen, and R. Yan, An analysis and mitigation of the reversal curse (2024), *arXiv:2311.07468 [cs.CL]*.
 - [20] P. Behnamghader, V. Adlakha, M. Mosbach, D. Bahdanau, N. Chapados, and S. Reddy, LLM2Vec: Large language models are secretly powerful text encoders (2024), *arXiv:2404.05961 [cs.CL]*.
 - [21] L. G. Charpentier and D. Samuel, GPT or BERT: why not both? (2024), *arXiv:2410.24159 [cs.CL]*.
 - [22] X. Yu, B. Guo, S. Luo, J. Wang, T. Ji, and Y. Wu, Antlm: Bridging causal and masked language models (2024), *arXiv:2412.03275 [cs.CL]*.
 - [23] H. Liu, X. Geng, L. Lee, I. Mordatch, S. Levine, S. Narang, and P. Abbeel, Towards better few-shot and finetuning performance with forgetful causal language models (2023), *arXiv:2210.13432 [cs.CL]*.
 - [24] H. Gisserot-Boukhlef, N. Boizard, M. Faysse, D. M. Alves, E. Malherbe, A. F. T. Martins, C. Hudelot, and P. Colombo, Should we still pretrain encoders with masked language modeling? (2025), *arXiv:2507.00994 [cs.CL]*.
 - [25] A. Paszke, S. Gross, F. Massa, A. Lerer, J. Bradbury, G. Chanan, T. Killeen, Z. Lin, N. Gimelshein, L. Antiga, A. Desmaison, A. Kopf, E. Yang, Z. DeVito, M. Raison, A. Tejani, S. Chilamkurthy, B. Steiner, L. Fang, J. Bai, and S. Chintala, Pytorch: An imperative style, high-performance deep learning library, in *Advances in Neural Information Processing Systems* **32** (Curran Associates, Inc., 2019) pp. 8024–8035.

- [26] W. Falcon and The PyTorch Lightning team, *PyTorch Lightning* (2019).
- [27] J. D. Hunter, Matplotlib: A 2d graphics environment, *Computing in Science & Engineering* **9**, 90 (2007).
- [28] T. pandas development team, *pandas-dev/pandas: Pandas* (2020).
- [29] Wes McKinney, Data Structures for Statistical Computing in Python, in *Proceedings of the 9th Python in Science Conference*, edited by Stéfan van der Walt and Jarrod Millman (2010) pp. 56 – 61.
- [30] C. R. Harris, K. J. Millman, S. J. van der Walt, R. Gommers, P. Virtanen, D. Cournapeau, E. Wieser, J. Taylor, S. Berg, N. J. Smith, R. Kern, M. Picus, S. Hoyer, M. H. van Kerkwijk, M. Brett, A. Haldane, J. F. del Río, M. Wiebe, P. Peterson, P. Gérard-Marchant, K. Sheppard, T. Reddy, W. Weckesser, H. Abbasi, C. Gohlke, and T. E. Oliphant, Array programming with NumPy, *Nature* **585**, 357 (2020).
- [31] Pivarski, Jim, Elmer, Peter, and Lange, David, Awkward arrays in python, c++, and numba, *EPJ Web Conf.* **245**, 05023 (2020).
- [32] J. Pivarski, I. Osborne, I. Ifrim, H. Schreiner, A. Hollands, A. Biswas, P. Das, S. Roy Choudhury, N. Smith, M. Goyal, P. Fackeldey, and I. Krommydas, *Awkward array* (2025).
- [33] A. Roy, J. Pivarski, L. Gray, C. Papageorgakis, M. Feickert, J. Duarte, H. Schreiner, R. Kansal, cmoore24 24, Sean github, K. W. Ho, K. Lieret, P. Fackeldey, and S. Rothman, *scikit-hep/fastjet* (2025).
- [34] M. Cacciari, G. P. Salam, and G. Soyez, FastJet User Manual, *Eur. Phys. J. C* **72**, 1896 (2012), [arXiv:1111.6097 \[hep-ph\]](https://arxiv.org/abs/1111.6097).
- [35] M. Huh, vqtorch: PyTorch package for vector quantization, <https://github.com/minyoungg/vqtorch> (2022).
- [36] F. Pedregosa, G. Varoquaux, A. Gramfort, V. Michel, B. Thirion, O. Grisel, M. Blondel, P. Prettenhofer, R. Weiss, V. Dubourg, J. Vanderplas, A. Passos, D. Cournapeau, M. Brucher, M. Perrot, and E. Duchesnay, Scikit-learn: Machine learning in Python, *Journal of Machine Learning Research* **12**, 2825 (2011).
- [37] T. Buss, *FLC-QU-hep/ranger-lite: RangerLite 1.0.0* (2025).
- [38] S. Chopra, H. Schreiner, E. Rodrigues, J. Eschle, and J. Pivarski, Vector: Jit-compileable mathematical manipulations of ragged lorentz vectors, *Journal of Open Source Software* **10**, 7791 (2025).
- [39] H. Qu, C. Li, and S. Qian, Jetclass: A large-scale dataset for deep learning in jet physics, [10.5281/zenodo.6619768](https://zenodo.org/record/6619768) (2022).
- [40] G. Kasieczka, T. Plehn, J. Thompson, and M. Russel, Top quark tagging reference dataset, [10.5281/zenodo.2603256](https://zenodo.org/record/2603256) (2019).
- [41] J. Alwall, R. Frederix, S. Frixione, V. Hirschi, F. Maltoni, O. Mattelaer, H. S. Shao, T. Stelzer, P. Torrielli, and M. Zaro, The automated computation of tree-level and next-to-leading order differential cross sections, and their matching to parton shower simulations, *JHEP* **07**, 079, [arXiv:1405.0301 \[hep-ph\]](https://arxiv.org/abs/1405.0301).
- [42] T. Sjöstrand, S. Mrenna, and P. Z. Skands, A Brief Introduction to PYTHIA 8.1, *Comput. Phys. Commun.* **178**, 852 (2008), [arXiv:0710.3820 \[hep-ph\]](https://arxiv.org/abs/0710.3820).
- [43] T. Sjöstrand, S. Ask, J. R. Christiansen, R. Corke, N. Desai, P. Ilten, S. Mrenna, S. Prestel, C. O. Rasmussen, and P. Z. Skands, An introduction to PYTHIA 8.2, *Comput. Phys. Commun.* **191**, 159 (2015), [arXiv:1410.3012 \[hep-ph\]](https://arxiv.org/abs/1410.3012).
- [44] J. de Favereau, C. Delaere, P. Demin, A. Giammanco, V. Lemaître, A. Mertens, and M. Selvaggi (DELPHES 3), DELPHES 3, A modular framework for fast simulation of a generic collider experiment, *JHEP* **02**, 057, [arXiv:1307.6346 \[hep-ex\]](https://arxiv.org/abs/1307.6346).
- [45] S. Chatrchyan *et al.* (CMS), The CMS Experiment at the CERN LHC, *JINST* **3**, S08004.
- [46] M. Cacciari, G. P. Salam, and G. Soyez, The anti- k_t jet clustering algorithm, *JHEP* **04**, 063, [arXiv:0802.1189 \[hep-ph\]](https://arxiv.org/abs/0802.1189).
- [47] G. Aad *et al.* (ATLAS), The ATLAS Experiment at the CERN Large Hadron Collider, *JINST* **3**, S08003.
- [48] A. van den Oord, O. Vinyals, and k. kavukcuoglu, Neural discrete representation learning, in *Advances in Neural Information Processing Systems*, Vol. 30, edited by I. Guyon, U. V. Luxburg, S. Bengio, H. Wallach, R. Fergus, S. Vishwanathan, and R. Garnett (Curran Associates, Inc., 2017).
- [49] M. Huh, B. Cheung, P. Agrawal, and P. Isola, Straightening out the straight-through estimator: Overcoming optimization challenges in vector quantized networks, in *Proceedings of the 40th International Conference on Machine Learning*, Proceedings of Machine Learning Research, Vol. 202, edited by A. Krause, E. Brunskill, K. Cho, B. Engelhardt, S. Sabato, and J. Scarlett (PMLR, 2023) pp. 14096–14113.
- [50] E. Buhmann, C. Ewen, G. Kasieczka, V. Mikuni, B. Nachman, and D. Shih, Full phase space resonant anomaly detection, *Phys. Rev. D* **109**, 055015 (2024), [arXiv:2310.06897 \[hep-ph\]](https://arxiv.org/abs/2310.06897).
- [51] J. Devlin, M.-W. Chang, K. Lee, and K. Toutanova, BERT: Pre-training of Deep Bidirectional Transformers for Language Understanding (2019), [arXiv:1810.04805 \[cs.CL\]](https://arxiv.org/abs/1810.04805).
- [52] K. He, X. Chen, S. Xie, Y. Li, P. Dollár, and R. Girshick, Masked autoencoders are scalable vision learners, in *Proceedings of the IEEE/CVF Conference on Computer Vision and Pattern Recognition (CVPR)* (2022) pp. 16000–16009.
- [53] H. Bao, L. Dong, S. Piao, and F. Wei, BEit: BERT pre-training of image transformers, in *International Conference on Learning Representations* (2022).
- [54] R. Wang, D. Chen, Z. Wu, Y. Chen, X. Dai, M. Liu, Y.-G. Jiang, L. Zhou, and L. Yuan, Bevt: Bert pretraining of video transformers, in *Proceedings of the IEEE/CVF Conference on Computer Vision and Pattern Recognition (CVPR)* (2022) pp. 14733–14743.
- [55] A. Baevski, W.-N. Hsu, Q. Xu, A. Babu, J. Gu, and M. Auli, data2vec: A general framework for self-supervised learning in speech, vision and language, in *Proceedings of the 39th International Conference on Machine Learning*, Proceedings of Machine Learning Research, Vol. 162, edited by K. Chaudhuri, S. Jegelka, L. Song, C. Szepesvari, G. Niu, and S. Sabato (PMLR, 2022) pp. 1298–1312.
- [56] C. Wei, H. Fan, S. Xie, C.-Y. Wu, A. Yuille, and C. Feichtenhofer, Masked feature prediction for self-supervised visual pre-training, in *Proceedings of the IEEE/CVF Conference on Computer Vision and Pattern Recognition (CVPR)* (2022) pp. 14668–14678.
- [57] J. Spinner, V. Bresó, P. de Haan, T. Plehn, J. Thaler, and J. Brehmer, Lorentz-Equivariant Geometric Algebra Transformers for High-Energy Physics, in *38th conference on Neural Information Processing Systems* (2024) [arXiv:2405.14806 \[physics.data-an\]](https://arxiv.org/abs/2405.14806).
- [58] J. Brehmer, V. Bresó, P. de Haan, T. Plehn, H. Qu, J. Spinner, and J. Thaler, A Lorentz-equivariant transformer for all of the LHC, *SciPost Phys.* **19**, 108 (2025), [arXiv:2411.00446 \[hep-ph\]](https://arxiv.org/abs/2411.00446).
- [59] M. Tschannen, C. Eastwood, and F. Mentzer, Givt: Generative infinite-vocabulary transformers (2024), [arXiv:2312.02116 \[cs.CV\]](https://arxiv.org/abs/2312.02116).
- [60] A. Radford, K. Narasimhan, T. Salimans, and I. Sutskever, Improving language understanding by generative pre-training (2018).
- [61] R. Xiong, Y. Yang, D. He, K. Zheng, S. Zheng, C. Xing, H. Zhang, Y. Lan, L. Wang, and T.-Y. Liu, On layer normalization in the transformer architecture, in *Proceedings of the*

- 37th International Conference on Machine Learning, ICML'20 (JMLR.org, 2020).
- [62] H. Touvron, M. Cord, A. Sablayrolles, G. Synnaeve, and H. Jégou, Going deeper with image transformers, in *Proceedings of the IEEE/CVF International Conference on Computer Vision (ICCV)* (2021) pp. 32–42.
 - [63] T. Darcet, M. Oquab, J. Mairal, and P. Bojanowski, Vision transformers need registers, in *The Twelfth International Conference on Learning Representations* (2024).
 - [64] S. Shleifer, J. Weston, and M. Ott, Normformer: Improved transformer pretraining with extra normalization (2021), [arXiv:2110.09456 \[cs.CL\]](https://arxiv.org/abs/2110.09456).
 - [65] L. Wright, Ranger - a synergistic optimizer., <https://github.com/lessw2020/Ranger-Deep-Learning-Optimizer> (2019).
 - [66] M. Zhang, J. Lucas, J. Ba, and G. E. Hinton, Lookahead optimizer: k steps forward, 1 step back, in *Advances in Neural Information Processing Systems*, Vol. 32, edited by H. Wallach, H. Larochelle, A. Beygelzimer, F. d'Alché-Buc, E. Fox, and R. Garnett (Curran Associates, Inc., 2019).
 - [67] L. Liu, H. Jiang, P. He, W. Chen, X. Liu, J. Gao, and J. Han, On the variance of the adaptive learning rate and beyond, in *International Conference on Learning Representations* (2020).

Appendix A: Model architecture and training details

1. Backbone architecture changes

Compared to OmniJet- α , which uses post-norm transformer blocks based on [60], we use pre-norm transformer [61] blocks in the backbone architecture as this choice is more common in modern transformer architectures. Furthermore, we add LAYERSCALE [62] to the architecture, but instead of initializing the per-channel weights with a small value as commonly done, we use a value of 1 as we found this initialization strategy to be more effective in practice in our trainings. We also add registers [63] to the backbone architecture which was found to slightly improve classification performance in initial studies. Overall we use a smaller backbone compared to OmniJet- α by using 8 transformer blocks with an embedding dimension of 128 instead of 3 transformer blocks with an embedding dimension of 256. Moreover, this leads to a much smaller backbone compared to the MPM work, which uses 8 transformer blocks with an embedding dimension of 512. The smaller model size in this work was chosen as we found that a larger backbone did not lead to better results in initial experiments. The token-ID-input backbone has 2.6 M parameters as opposed to 4.5 M parameters in the original OmniJet- α work. The number of parameters is further reduced in the continuous-input backbone, which has 1.6 M parameters. The much larger number of parameters in the token-ID-input case is due to the trainable token embedding layer for the token-ID input (which maps 8192 token-IDs to the embedding dimension 128 of the backbone), resulting in around 1 M additional parameters. Finally, the backbone model is conditioned on the number of particles, as the continuous-input generative model was found to struggle with correct end token prediction when not using this conditioning in early tests. For the case where the model acts as a generative model, we

fit a kernel density estimate (KDE) on the distribution of the number of particles per jet, from which we sample to generate the conditional information for jet generation³. We combine jet-level information (i.e. the number of particles) with the per-particle information by first projecting both the jet-level and the particle-level feature vectors with a linear layer to the embedding dimension of the backbone, and then adding the jet-level embedding to each particle embedding. The details of the backbone architecture and hyperparameter choices are listed in Table I. Due to computational constraints, no dedicated hyperparameter optimization was performed. Instead, a few configurations were tested, and we selected configurations that were found to lead to stable training performance while also not requiring an unnecessarily large model.

2. Token prediction head

As in the original OmniJet- α work, we use a linear layer to project the backbone output to the logits of the token-IDs when training on the NTP target only. The token prediction head used for MPM, as well as the token prediction head used for the NTP prediction in the joint pre-training consists of two transformer blocks with the same embedding dimension as the backbone, followed by a linear layer to obtain the masked and next token logits, respectively.

3. Classification head

Compared to OmniJet- α we adapt the classification head to feature two class-attention blocks [10, 62] followed by a linear layer (instead of two linear layers with a summation over all particles between them) to obtain a more capable classification head. Furthermore, we do not apply the causal mask in the backbone in classification mode as this is an unnecessary restriction on the model's capacity when trained for classification. The classification head adds another 400 k parameters to the model, leading to a total of 2 M trainable parameters in the continuous-input classifier, which is similar in size to the OmniLearn [11, 12] or ParT [10] models.

4. VQ-VAE architecture changes

As the hybrid setup with continuous input and token-ID prediction requires on-the-fly decoding of token-IDs during the generation loop, the VQ-VAE has to be trained with a causal mask in the decoder. Additionally, we use the same transformer block architecture as in the backbone model, instead of the NormFormer [64] architecture that was used in OmniJet- α . The vector quantization is implemented using the vqtorch [35] library. The VQ-VAE hyperparameters are

³ The generated values from the KDE are clipped to be larger than zero and subsequently rounded to the closest integer number.

listed in Table II. As for the backbone, no dedicated hyperparameter tuning was performed, rather, a few configurations were tested and found to lead to stable results.

5. Training details

All models are trained with the Ranger [65] optimizer, which uses the Lookahead [66] optimizer with RAdam [67] as the inner optimizer. A constant learning rate of 1×10^{-3} and a batch size of 1000 is used for all trainings except for trainings where we use 10k jets or less, for which we use a batch size of 100. Pre-trainings are performed for a total of 1 M steps, with the final model state being used for evaluation. Classification trainings are performed for up to 1 M steps as well, but with early stopping based on the validation loss. Classification runs are repeated with five different random seeds and the average and standard deviation of the five runs is reported. The model state with the lowest validation loss is used for evaluation in classification runs.

TABLE I. Backbone model hyperparameters

Hyperparameter	Value
Number of transformer blocks	8
Embedding dimension	128
LAYERSCALE initialization value	1.0
Optimizer	Ranger [65–67]
Learning rate	0.001
Batch size (if $N_{\text{train}} > 10\,000$)	1000
Batch size (if $N_{\text{train}} \leq 10\,000$)	100

Appendix B: Performance of the VQ-VAE

A comparison of both particle-level and jet-level features of the original JetClass dataset and the distributions obtained after tokenization (and subsequent decoding with the VQ-VAE

TABLE II. VQ-VAE model hyperparameters. For further information on α , β and ν see [35, 49].

Hyperparameter	Value
Number of transformer blocks (encoder)	4
Number of transformer blocks (decoder)	4
Embedding dimension	128
LAYERSCALE [62] initialization value	1.0
Optimizer	Ranger [65–67]
Learning rate	0.001
Batch size	1000
Codebook size	8 192 (kin.) 32 768 (ext.)
α	10
β	0.9
ν	1
Replacement frequency	500 steps

decoder) are shown in Figure 7. As can be seen in the distribution of the trajectory displacement d_0 , the VQ-VAE struggles to accurately reproduce this distribution. We found this feature to be very challenging to encode with a VQ-VAE, given that it features a very sharp peak at 0 with long tails towards small and large values. However, we leave further studies regarding high-resolution tokenization of those features for future work.

Appendix C: Extending the feature set

To further improve the performance and utility of our models, we extend the input feature set of our model. We add the particle mass as well as the particle-ID and the trajectory displacement features to the input feature set of the model. A new VQ-VAE is trained for the extended feature set, using a codebook size 4 times larger than for the standard feature set, and a model is subsequently pre-trained with next token prediction.

The generative performance obtained with the two different input feature sets is shown in Figure 8, which shows the particle p_T and two of the newly added features, the particle charge and the transverse impact parameter d_0 , as well as several jet level features. The two dotted reference lines in Figure 8 correspond to the different VQ-VAEs used for the two different feature sets, leading to slightly different target distributions during the generative training.

The model trained on the extended feature set shows similar performance on observables related to the kinematics of the particles (both on particle- and jet-level). The smoother distribution of the particle p_T in the extended feature set case arises from the VQ-VAE having a larger codebook size. Both the particle charge distribution and the d_0 distribution show good agreement with the corresponding target distribution.

By extending the input feature set, the classification performance is drastically improved as can be seen in Figure 9. This overall improvement is expected as those features are known to be useful for jet tagging. The performance when trained on the whole JetClass dataset using the extended feature set leads to an accuracy of 85.7% in the baseline case whereas the kinematics-only model reaches an accuracy of only 70%. Generative pre-training leads to a notable improvement in classification performance for dataset sizes up to 1 M jets when using the extended feature set. For larger training dataset sizes, the performance of the pre-trained model converges to the performance of the from-scratch model.

Appendix D: Fine-tuning with fixed backbone representations

To investigate how aligned the pre-trained backbones are with the classification task, we perform classification fine-tuning where we only train the classifier head, shown in Figure 10. While MPM and the joint pre-training perform better or on-par with the baseline model (in which also the backbone weights are allowed to change during training) for all dataset sizes, this is not true for MPM-Causal, which is outperformed

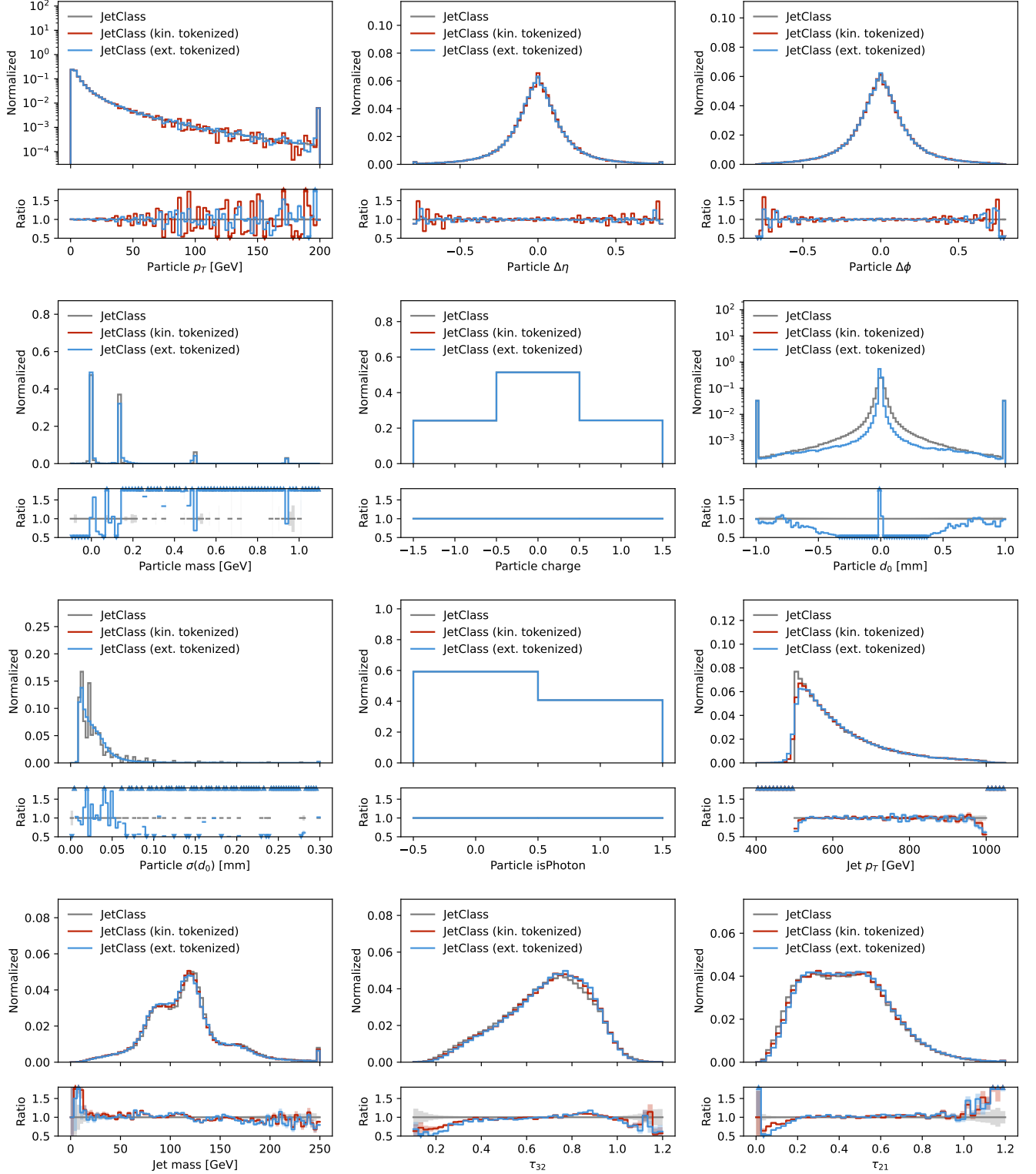


FIG. 7. Comparison of the original JetClass dataset and the corresponding distributions obtained after tokenization. The tokenized datasets are the target for the generative models for the two feature sets investigated in this work: kinematics-only (kin.) and the extended feature set (ext.). Particle features related to trajectory displacement (d_0 and $\sigma(d_0)$) are only shown for charged particles.

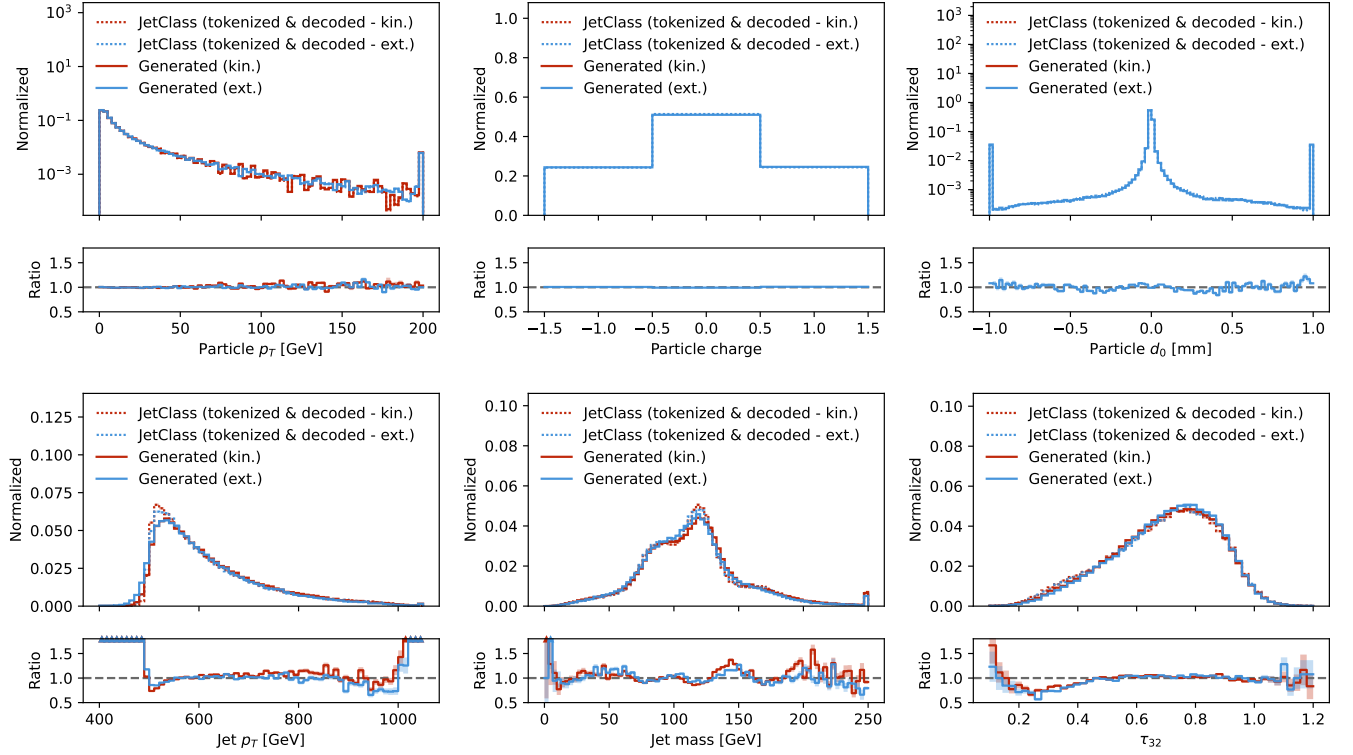


FIG. 8. Comparison of the jets that are generated by the continuous-input model using the kinematics-only (kin.) and the extended feature set (ext.). The dotted lines show the distributions obtained from tokenization and subsequent decoding of the JetClass dataset with the corresponding VQ-VAE. The solid lines show the distributions obtained from the generative models. The ratio panels show the ratio between the distribution obtained from the generative model and the corresponding target distribution (which is shown in the same color in dotted linestyle).

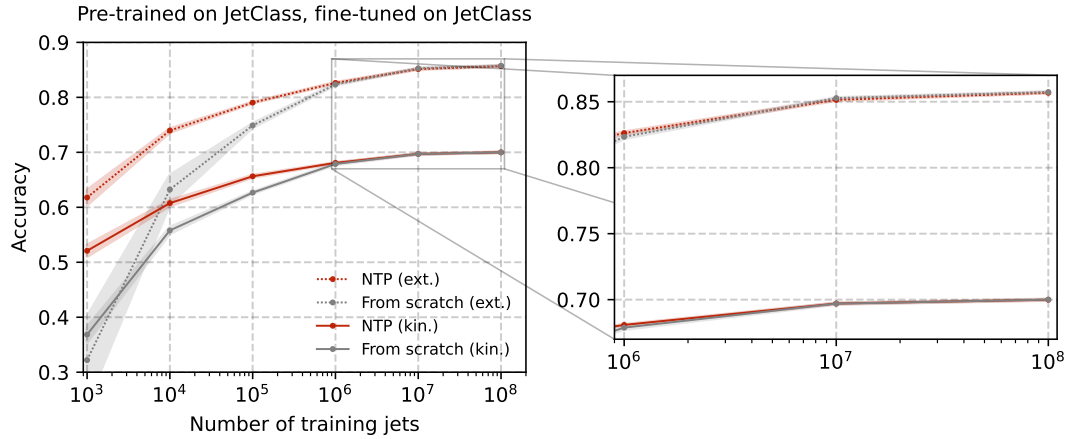


FIG. 9. Multi-class classification performance on the JetClass dataset (all 10 jet types) as a function of the number of training jets comparing the different pre-training strategies with the corresponding from-scratch baselines for the kinematics-only (solid) and the extended feature set (dotted).

by the from scratch model at a dataset size of 1.2 M training jets. Even more notable is the behavior for the model that is pre-trained with NTP: this model is outperformed for the whole training dataset range, meaning that this backbone rep-

resentation does not offer an advantage over the baseline when

the weights are not adapted during fine-tuning.⁴

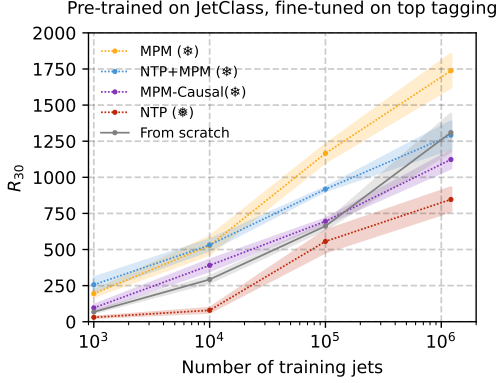


FIG. 10. Classification performance on the top tagging dataset when fine-tuning with a fixed backbone.

In order to explore this behavior in more detail, we study the gradients, validation loss and validation R_{30} for the different setups. Figure 11a (left) shows the norm of the gradient of the backbone model for the individual runs from Figure 10 at a dataset size of 10 000 jets. The backbone model obtained from NTP pre-training shows drastically larger gradients compared to the other methods. MPM, MPM-Causal and NTP+MPM have larger gradients than the from-scratch baseline (where the backbone is allowed to change) indicating that there remains significant gradient signal to update the frozen weights. However, those models still converges to a lower validation loss, as shown in Figure 11a (middle). This is not true for the NTP model, which indicates that the representations obtained

from this pre-training are not as aligned with the classification task as the ones of the other methods, or at least is less suited for subsequent fine-tuning to classification in a model with bi-directional attention model. We note that by switching from causal attention during pre-training to bi-directional attention during fine-tuning, the fixed representation is being used in a way that it was not trained for. And since it is fixed, it is not able to adapt. Figure 11b shows the corresponding behavior when using causal attention in the classifier training. The fine-tuning of the NTP-pre-trained model is significantly more stable, with the loss decreasing faster and smoother. Furthermore, the gradients show a similar behavior as the fine-tuning of the MPM-Causal backbone. This supports the hypothesis above, that the directionality is an important component contributing to the performance loss. However, it is not a complete explanation as the fixed NTP backbone still lead to worse classification performance in this scenario. We hypothesize that the reason for this is that the output representation of the fixed NTP backbone will be too strongly aligned to the generative task making it more difficult to adapt to the classification task. In order to investigate whether this can be mitigated, we compare fine-tunings with both fixed and trainable backbones for the default case where the NTP head is just a single linear layer to fine-tunings where the NTP head contains two transformer blocks and a subsequent linear layer like the MPM head. The classifier architecture is the same in all cases, only the head during pre-training differs between the different approaches. As shown in Figure 12, while the performance with the fixed backbone improves, both pre-training architectures perform similarly in the subsequent fine-tuning when the backbone weights are allowed to change as well.

⁴ This effect did not show up in the original OmniJet- α work, which used token-IDs as input rather than the continuous feature vector input used here. We believe that the baseline model in that case struggles with classification because it also needs to “decode” the information contained in

the token-IDs. The pre-training likely performs some of this decoding while training on the generative task, allowing it to outperform the baseline model. Using continuous input allows the classifier to completely bypass the token-IDs, making this baseline model more capable compared to that of [9].

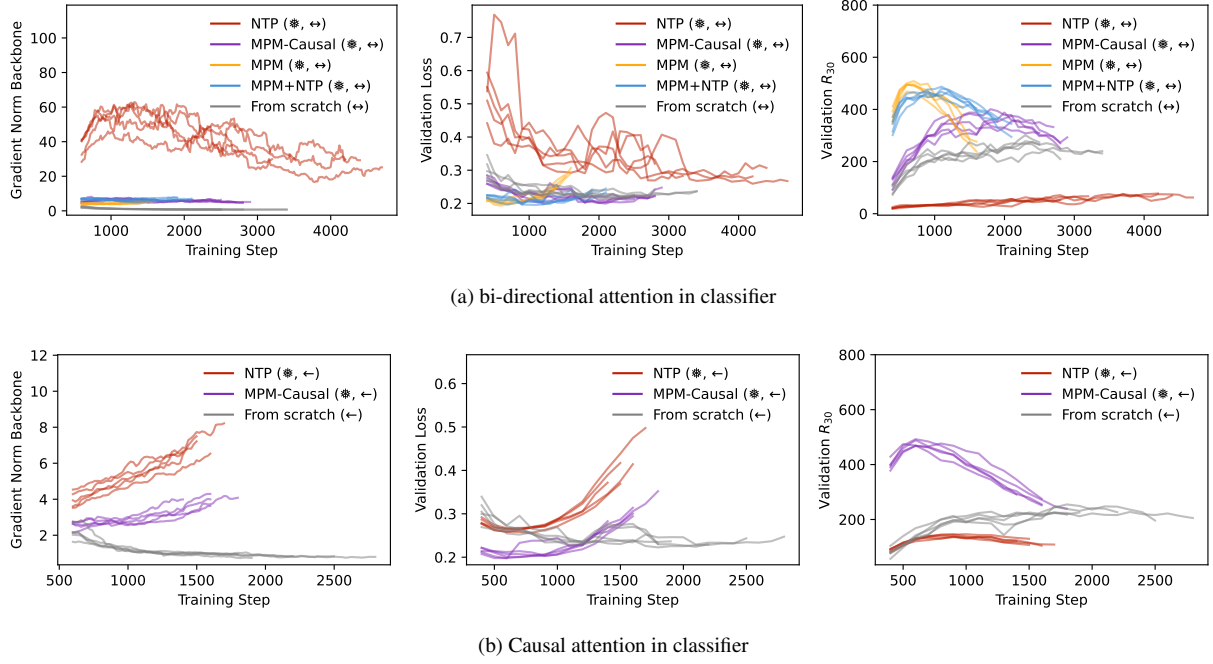


FIG. 11. Evolution of the backbone’s gradient norm, as well as the validation loss and R_{30} as a function of the training step. For each pre-training strategy five different runs are shown, corresponding to the five different runs with 10 000 training jets in Figure 10. The snowflake symbol indicates that the weights of the backbone are fixed. The left-right arrow in the legend indicates that bi-directional attention is used in the backbone whereas a left arrow indicates that attention is only allowed to previous particles in the sequence (i.e. causal attention). The rolling average is shown for better readability. We show the average of the last 30 logged values of the gradients, which are logged every 20 training steps, and the average over the last 4 epochs for the validation loss and validation R_{30} .

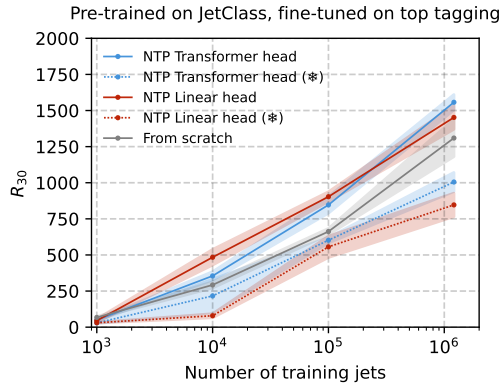


FIG. 12. Classification performance on the top tagging dataset for NTP pre-trained models with two different architectures in the model head: *Linear head* corresponds to the model head being a single linear layer, whereas *Transformer head* corresponds to a model head with two transformer blocks and a linear layer.